

Simulation of Flow and Heat Transfer of Humid Air in Spent Fuel Cooling Ponds

Ahmed Ramadan, Reaz Hasan* and Jenna Tudor

Abstract— This paper reports a CFD investigation on flow and heat transfer of the humid air which circulates above water ponds in large installations such as spent nuclear fuel cooling ponds. The numerical methodology involves a 3-cell zone approach to enable evaporative boundary condition to be implemented. Calculations are carried out for seasonal variations of temperature and humidity which show the contributions of sensible and latent heat losses. The results presented in this paper provide useful insights into the flow development and heat transfer mechanisms present. The results may be of use in the design of ventilation systems and the description of the methodology may be useful to practitioners wishing to carryout similar investigations.

Index Terms—Cooling pond, heat loss, humid air, CFD

I. INTRODUCTION

In many water pool applications such as swimming pools and Spent Nuclear Fuel (SNF) ponds [1], evaporation from the free water surface plays a vital role in establishing the heat transfer and flow field. Detailed data for overall flow field and heat transfer are needed for more power efficient swimming pool design [2], and obtaining a longer and safer operation condition for SNF ponds [3]. Hence it is very important to understand the mechanism of humid air distribution to be able to evaluate the amount of heat and mass loss from such ponds.

Establishing a valid numerical model using CFD is the main objective of this work in order to simulate the vapour movement and to estimate the heat transfer in terms of sensible and latent heat. Furthermore, a parametric study on the effect of the seasonal climate on flow field and heat transfer process will be performed based on the typical UK average weather conditions. The introduced methodology indicates that CFD can be a reliable tool to offer a very realistic simulation which can lead to deeper understanding of complex water vapour behaviour. Also, the method can be used to evaluate the amount of heat transfer to provide data for assisting in ventilation system design and the risk associated with the excessive heating for SNF ponds.

The model is an extension of our previous work presented earlier [1] and consists of two water pools connected to each

other by a narrow bypass. The main difference in the present investigation is that we have now focused our attention on the volume of air on top of the water surface and have included a ventilation inlet and outlet Fig. 1. Also, the geometry is a scaled down version of the SNF pool to aid us in establishing the methodology. These ponds can be described as a large water basin with concrete walls and floor, where the evaporation takes place from the free heated water surface. These two ponds are covered by a concrete building.

In this paper, we propose a 3-cell zone approach to implement evaporative boundary condition. After a careful validation exercise we have performed parametric studies on flow and heat transfer for various seasonal data. Although the calculations were carried out in the context of SNF, the methodology is equally applicable for similar other applications such as leisure swimming pools.

II. METHODOLOGY

A. Steady State Simulation

Steady state simulation was accomplished using the commercial CFD package of ANSYS FLUENT 14.5 [4]. The general methodology is well established and can be found in many textbooks such as Versteeg et al. [5]. Navier-Stokes equations were solved using the SIMPLE algorithm. In addition, energy equations were solved to take into account the heat transfer and buoyancy forces were enabled through momentum equations. Since the air considered is humid, species transport (scalar) equation has also been solved. In order to add the turbulence effect, the k - ϵ model with standard wall functions has been used.

The boundary condition at the ventilation inlet was defined as a uniform velocity with magnitude of 0.8 m/s in X-direction (representing 0.224 Air Change per Hour, ACH), and temperature equal to the ambient value. The outflow boundary condition was imposed at ventilation exit. For wall surfaces, the convection boundary condition was applied with heat transfer coefficient of 0.25 W/m²-K. The side and bottom walls of the vapour source zone were considered to be at constant temperature of 26 °C which was the same as the water temperature. For all the solid zone surfaces the no-slip boundary condition was employed.

Non-uniform hexahedral mesh was generated to discretise the domain and a typical grid distribution is shown in Fig. 2. The grids were concentrated in areas of steep gradients and, after a few trials, approximately 0.5 million cells were found

Manuscript received March 17 2014; revised April 1 2014

R. Hasan is with the University of Northumbria, Newcastle, NE1 8ST, UK (corresponding author to provide phone: 0191 243 7233; fax: 0191 227 3684; (e-mail: reaz.hasan@northumbria.ac.uk).

J. Tudor is with the University of Northumbria, Newcastle, NE1 8ST, UK (e-mail: jenna.tudor@northumbria.ac.uk).

A. Ramadan was a student with the University of Northumbria, Newcastle, NE1 8ST.

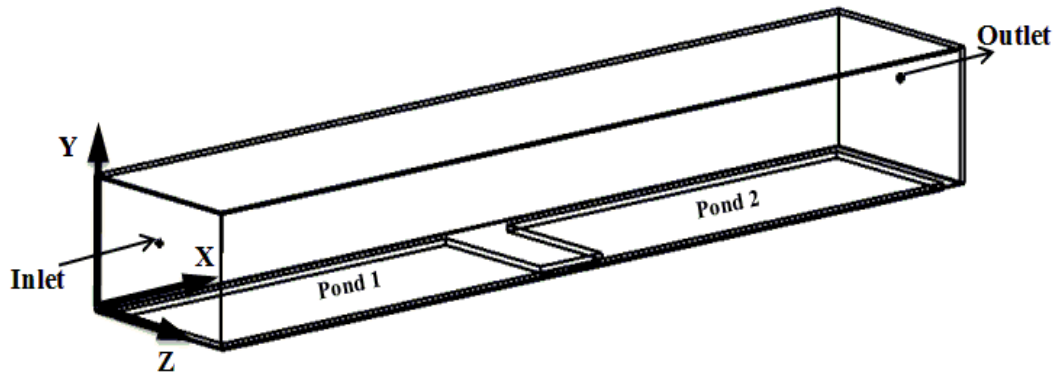


Fig. 1. The 3-D sketch for computational domain.

to yield satisfactory results (that were fairly insensitive to further resolution) and hence has been used for all the calculations presented in this paper. For convection terms, second order upwind differencing has been followed. A typical computational time on a single Intel core 2Duo E6600 2.4 GHz processor took about 4 hours in order to achieve the convergence residual of 10^{-4} .

B. Implementation of multi-zone flow model

A multi-zone flow model has been incorporated into the simulation which is explained by reference to Fig. 3 below. We have considered the domain to consist of three cell zones: solid zone for the walls, vapour zone for the water vapour source and humid air zone. Inclusion of these three zones allows us to implement the boundary conditions in a very realistic way and also enables us to include variation of ambient conditions for different seasons.

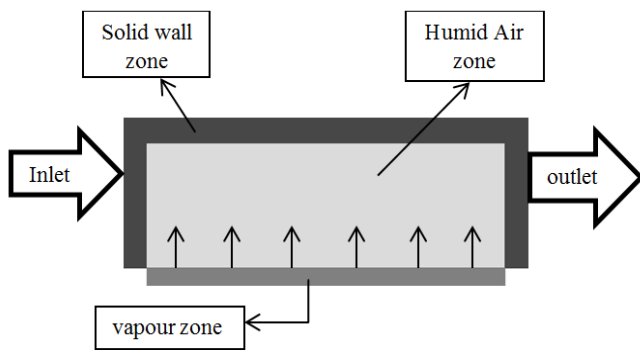


Fig. 3. Schematic of the three domains.

For the solid zone, the walls were considered to be made of concrete with thermal conductivity of 1.4 W/m-K. The vapour zone is a very thin zone (typically three layers of

cells) which represents the boundary layer just above the water surface. Air is considered to be fully saturated with water vapour at that temperature. This thin boundary layer was introduced to the continuity equation (1) as mass source term S_m with water vapour mass flow rate of $m = m_o - m_i$, where m_i represents the absolute humidity at entry (determined from ambient condition) and m_o represents the absolute humidity at exit (assumed fully saturated).

$$\frac{\partial \rho}{\partial t} + \nabla \cdot (\rho \vec{v}) = S_m \quad (1)$$

To maintain dimensional homogeneity, the mass source term is obtained by (2), where V represents the cell zone volume.

$$S_m = \frac{m \cdot}{V} \quad (2)$$

III. VALIDATION OF THE METHODOLOGY

The methodology described above was validated against the published work of Li et al. [6]. The flow domain involved the movement of humid air in a swimming pool of practical size (22.5m x 9m x 7.5m). Most simulation boundary condition and geometry details were available and implemented in our computations. Figs. 4 and 5 show the comparisons of temperature and relative humidity (RH) distributions on the same scale (both shown in grayscale). Reasonable agreements can be seen for both plots and the differences may be attributed to slight uncertainty in geometry specification [6] and turbulence models.

IV. RESULTS AND DISCUSSION

Calculations were carried out for four different seasonal variations and the results were analysed by plotting velocity,

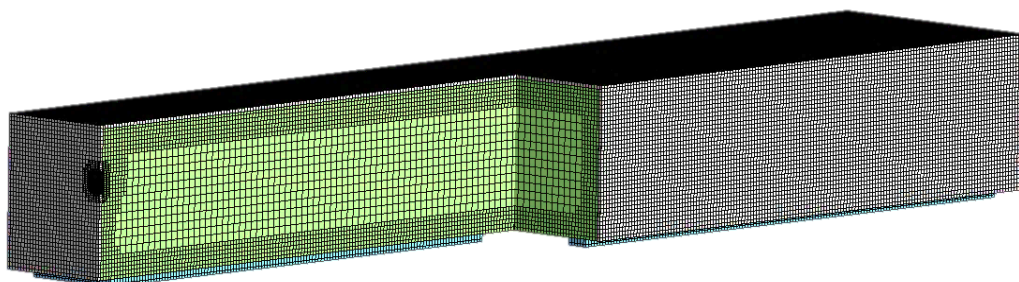


Fig. 2. Section view of grid distribution for computational domain.

temperature, relative humidity and integral values of latent and sensible heats. Typical flow fields for winter conditions (temperature: 5°C and RH:85%) are presented and discussed in this section.

A. Velocity

Fig. 6. Shows the streamlines of humid air on the Z-mid plane and shows a number of vortical structures. The first vortex is due to the interaction between the incoming ventilation air with buoyancy driven flow due to heat released from the water surface. On the other hand, the central counter-rotating vortices are a direct manifestation of the current geometry where there is an ‘inactive’ separation region between the two ponds. The other vortex near the exit is just opposite to the inlet vortex. The velocity contours in Fig. 7 clearly show that magnitudes are very small and most of the higher velocities are concentrated near the boundaries.

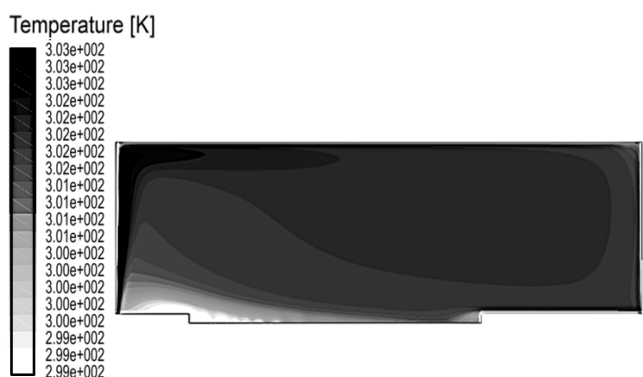


Fig. 4(a). Temperature distribution for the present method.

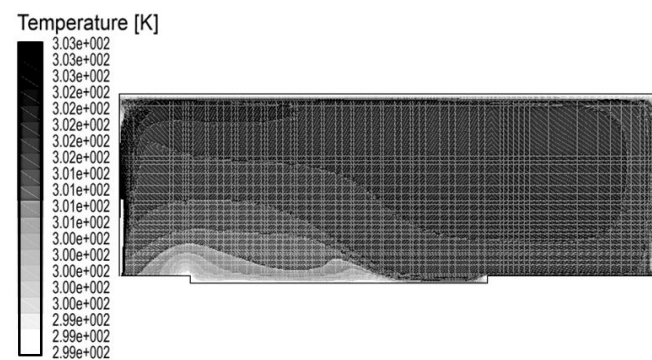


Fig. 4(b). Temperature distribution for Li et al. [6]

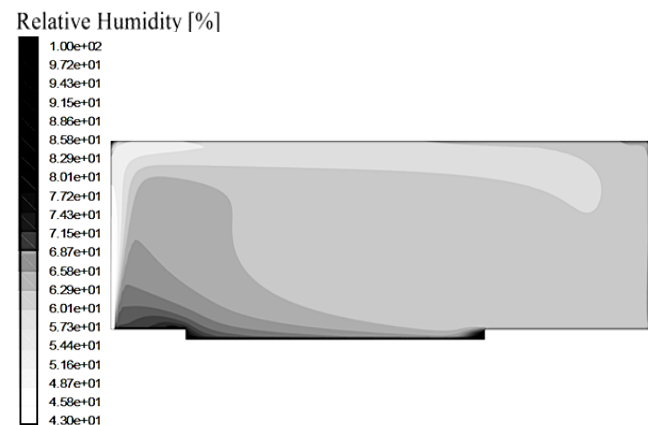


Fig. 5(a). RH contour for the present method

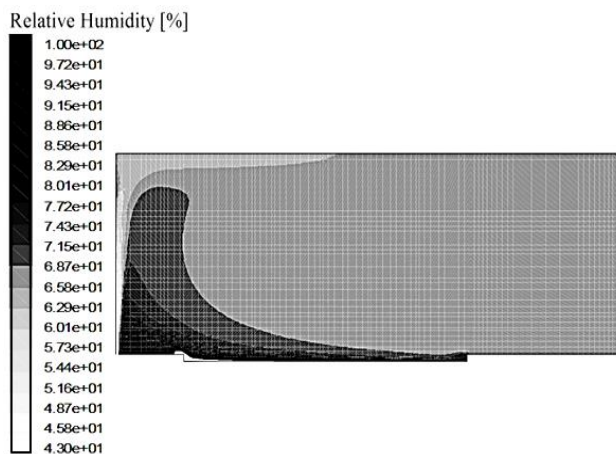


Fig. 5(b). R.H contour for Li et al. [6]

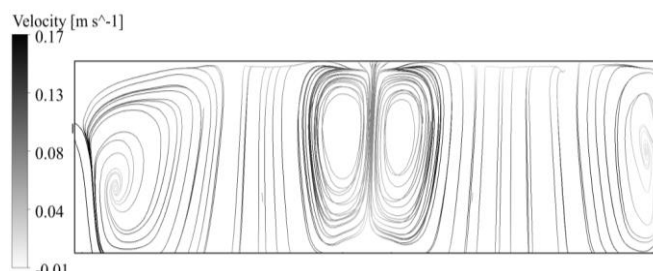


Fig. 6. Streamlines on z- mid plane (aspect ratio modified for clarity).

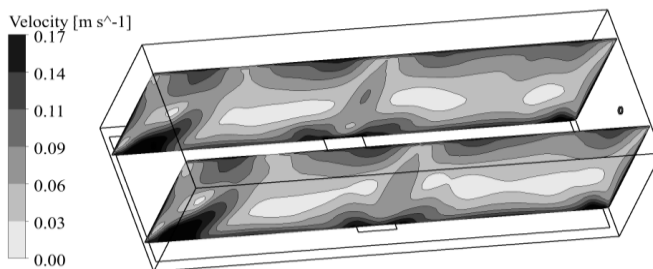


Fig. 7. Velocity contours on Z-0.4 and Z-2.3 planes.

B. Temperature

Temperature profiles at a few chosen locations in the X-direction and along the Z-mid plane are shown in Fig. 8. It can be observed that the temperature is slightly higher above the water surface than at other places. The effect of the geometry is visible on the X-mid plane.

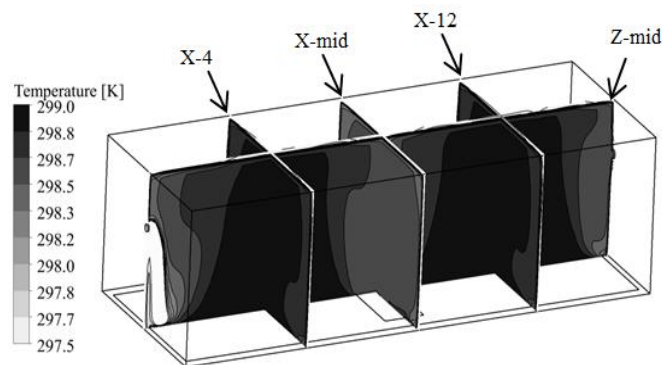


Fig. 8. Temp. contours on Z-mid, X-4, X-mid and X-12 planes.

C. Relative humidity

Figs. 9 and 10 illustrate the relative humidity distribution in the X-direction as well as on the Z-mid plane. The rise of water vapour from the saturated vapour zone is clearly visible and as it moves upward, a plume of constant high RH zone is observed. Interestingly, the lower values of RH display a ‘mushroom’ shape due to interaction with the ceiling. The RH plots in Fig. 10 shows the distributions on three Y-planes and are in line with the previous plots.

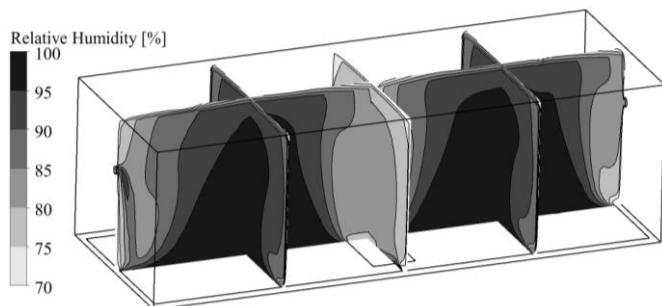


Fig. 9. R.H. contours on Z-mid, X-4, X-mid, and X-12.

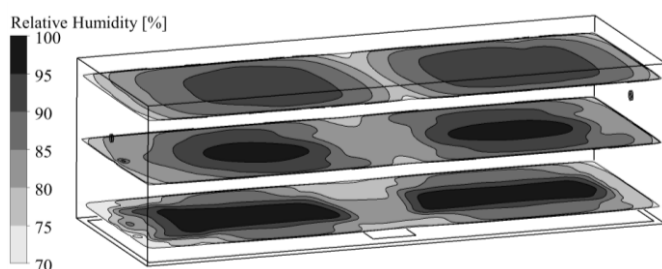


Fig. 10. R.H. contours on Y-0.2, Y-1 and Y-1.8.

D. Parametric study

Heat losses through the building were split as sensible and latent heats and were calculated for different seasonal variations. The climatic data were incorporated through ambient air temperature and relative humidity as shown in Table 1.

E. Seasonal comparison of Heat loss

A comparison of heat loss was conducted for four seasons and Fig. 11 illustrates the amount of heat loss from the building body in the form of sensible and latent heat. It can be clearly seen that the outdoor temperature variation has a significant effect on the total heat loss through sensible heat. On the other hand, the moisture content has relatively lesser effect but still is significant and varies from 18% to 33% of the total heat loss. We have carried out further parametric studies by varying the inlet velocity (i.e. ACH) and it was found that the loss due to latent heat is almost directly proportional to the ACH while sensible heat loss is rather insensitive.

Since the evaporation rate is highly dependent on ambient air temperature and relative humidity [7, 8], a scenario as in summer configuration, where the ability of the building to discharge heat is reduced, might cause a drop in the evaporation rate. Hence the cooling performance in such ponds would be reduced and would require less energy.

However, for SNF cooling ponds, this observation may be a cause for concern because it may lead to an undesirable increase of temperature of the water in which the spent fuels are kept immersed.

F. Thermal stratification

TABLE I
Effect of seasonal atmospheric condition on heat transfer and temperature stratification.

Season	Temp. (°C)	RH (%)	Strat. Level (°C)	Sensible heat loss (W)	Latent heat loss (W)
Winter	5	85	0.65	625.3	313
Spring	15	60	0.36	326.2	73
Summer	20	76	0.2	177.5	75
Autumn	10	87	0.5	475.4	232

Fig. 12 shows the vertical temperature gradient on the Z-mid plane at different X-positions along the length of the pool. Except positions X-1 and X-15 which are affected by proximity to inlet and outlet respectively, the curves display a very slight drop in bulk temperature. Based on the volume averaged temperature very near to the ceiling and that on the water surface, we have noted slight temperature stratification and the values are shown in Table 1. Also shown on this Table are the numerical values of sensible and latent heat quantities.

Further parametric studies were carried out by varying the ventilation inlet and outlet conditions in terms of their location and ACH. As expected, very significant variations were observed and our findings were mostly in line with those reported by Said et al. [9] which indicates that opening the building doors is the main cause in change of the temperature. In the present case, ventilation inlet and outlet can be assumed to have the similar effect. For instance, Fig. 13 illustrates the affect in the temperature distribution by increasing the ventilation inlet velocity to 5 m/s.

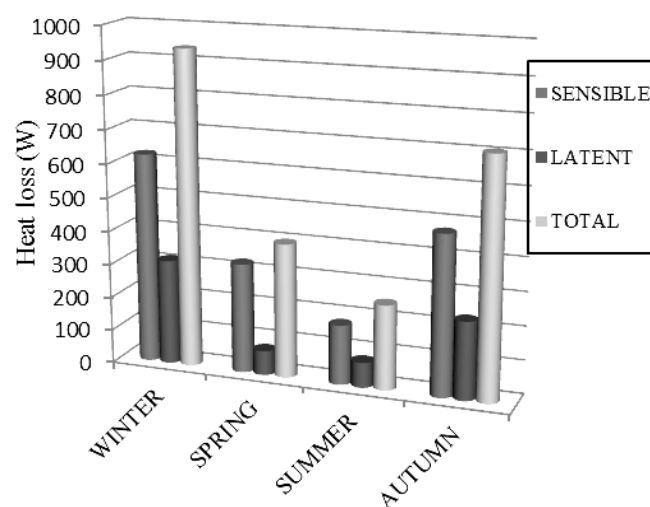


Fig. 11. Sensible and latent heat loss variation under different ambient conditions.

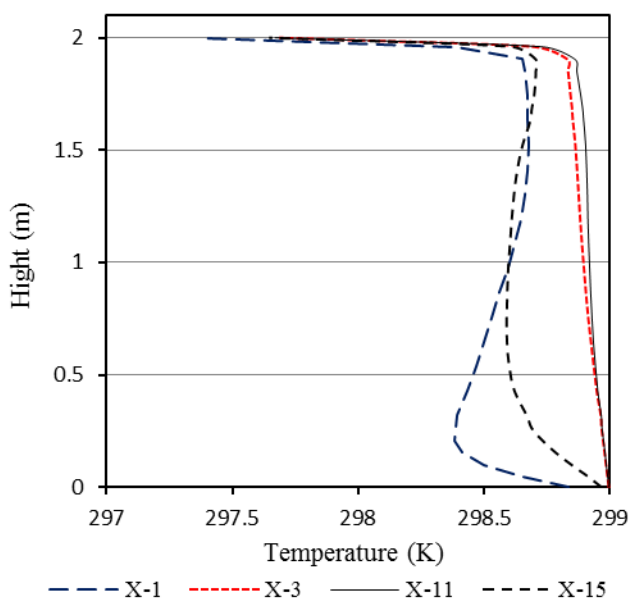


Fig. 12. Vertical temperature gradient on Z-mid plane.

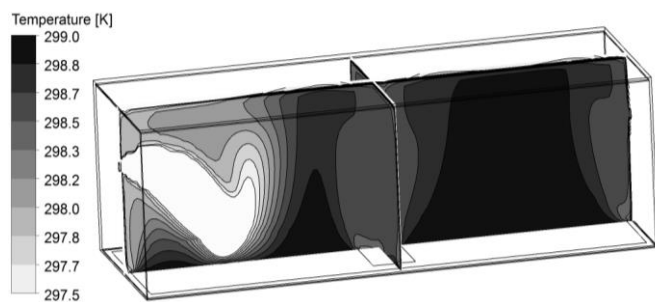


Fig. 13. Temperature gradient on Z-mid and X-mid planes for inlet of 5 m/s.

- [3] Kozlov, Y.V., et al., *Long-term storage and shipment of spent nuclear fuel*. Atomic Energy, 2000. **89**(4): p. 792-803.
- [4] ANSYS FLUENT 14.5 (2014).
- [5] Versteeg, H.K. and W. Malalasekera, *An introduction to computational fluid dynamics: the finite volume method*. 2007: Pearson Education.
- [6] Li, Z., *CFD Simulations for Water Evaporation and Airflow Movement in Swimming Baths*. VENTInet, 2005(14): p. 10-11.
- [7] Vinnichenko, N.A., et al., *Direct computation of evaporation rate at the surface of swimming pool*. Recent Researches in Mechanics, 2011, 2011: p. 120-124.
- [8] M. D. Hancock, "Indoor swimming pools and leisure centres – A model to improve operational effectiveness and reduce environmental impact," *CIBSE Technical Symposium, Sept. 6-7, 2011, De Montfort University, Leicester, UK*.
- [9] Said, M., R. MacDonald, and G. Durrant, *Measurement of thermal stratification in large single-cell buildings*. Energy and buildings, 1996. **24**(2): p. 105-115.

V. CONCLUSION AND FUTURE WORK

- 1) Employing the three cell zones in the model allows for implementing the boundary conditions in a very realistic and generalised way.
- 2) The model can be used to predict both sensible and latent heat for different seasonal conditions.
- 3) Temperature stratification in the vertical direction has been found to be small but not insignificant.
- 4) The boundary conditions need further improvement. This can be done by considering condensation on the walls.
- 5) In order to get more realistic simulation for specific applications, accurate data about operational and environmental conditions needs to be collected.
- 6) Having established the methodology, work is currently underway to simulate the flow and heat transfer on a full scale model of SNF pond.

REFERENCES

- [1] Robinson, P., R. Hasan, and J. Tudor. *Numerical Simulation of Flow and Heat Transfer in Spent Fuel Cooling Ponds*. in Lecture Notes in Engineering and Computer Science: *Proceedings of the World Congress on Engineering*. 2013, pp. 1861-1864.
- [2] Shah, M.M., *Prediction of evaporation from occupied indoor swimming pools*. Energy and buildings, 2003. **35**(7): p. 707-713.